Comparative Analysis of Thermoregulation Models to Assess Heat Strain in Moderate to Extreme Heat

Ankit Joshi,[1,2] Bryce Twidwell,[1] Michael Park,[1] and Konrad Rykaczewski[1,2*]*

1. *School for Engineering of Matter, Transport and Energy, Arizona State University, Tempe, AZ 85287, USA*
2. *Julie Ann Wrigley Global Futures Laboratory, Arizona State University, Tempe, AZ 85287, USA*

Corresponding authors:

Konrad Rykaczewski, Ph.D.	Ankit Joshi, Ph.D.
Associate Professor	Assistant Research Scientist
Arizona State University	Arizona State University
777 E. University Dr.	777 E. University Dr.
Tempe, AZ 85281	Tempe, AZ 85281
Email: konradr@asu.edu	Email: ankit.joshi@asu.edu

ORCIDs:

Ankit Joshi: 0000-0002-5399-1069

Konrad Rykaczewski: 0000-0002-5801-7177

Acknowledgement: This research was supported by the National Science Foundation Leading Engineering for America's Prosperity, Health, and Infrastructure (LEAP HI) #2152468 award.

Competing Interests: The authors have no relevant financial or non-financial interests to disclose.

Abstract

As global temperatures rise due to climate change, the frequency and intensity of heatwaves are increasing, posing significant threats to human health, productivity, and well-being. Thermoregulation models are important tools for quantifying the risk of extreme heat, providing insights into physiological strain indicators such as core and skin temperatures, sweat rates, and thermal comfort levels. This study evaluated four thermoregulation models of varying complexity, differentiated by the geometry and underlying thermoregulatory mechanisms. The models assessed include the Gagge two-node model, the Stolwijk-1971 model, the JOS3 model, and the UTCI-Fiala model. Additionally, we introduce the Stolwijk-2024 model, a modified version of the original Stolwijk model, which incorporates updated empirical coefficients derived from recent studies while retaining the original framework. The models were tested against human trial data across a wide range of extreme heat exposures, including transient extreme heat, humid heat, various physical activity levels, and clothing insulation scenarios. Our findings demonstrate that multi-node and multi-segment models, such as JOS3, UTCI-Fiala, and Stolwijk-2024, reliably predict core (average RMSD: <0.3°C) and skin (average root-mean-square deviation, RMSD: <0.6°C) temperatures, making them suitable for assessing heat strain and thermal comfort in moderate to extreme environmental conditions. In contrast, simpler models like the single-segment, two-node Gagge's model performed poorly in predicting core temperature under conditions involving high metabolic rates (>3.75 met) in moderate to hot environments (>35°C), with an average RMSD of 1.2°C. Similarly, the Stolwijk-1971 model showed a systematic bias (~0.45°C), underpredicting core temperatures during high metabolic rates. This study underscores the robustness and applicability of open-source models like JOS3 and Stolwijk-2024 in public health, urban design, and climate impact research, highlighting their potential to improve our understanding of heat strain and thermal comfort in the context of a warming climate.

Highlights

- Comprehensive validation of thermoregulation models under extreme climate
- Updated Stolwijk model has enhanced accuracy in predicting core and skin temperatures
- Two-node or overly simplified models can underperform in analyzing heat exposures

Keywords: Thermoregulation model, Model evaluation, Comparative analysis, Extreme heat exposure, Heat strain assessment

1.Introduction

As global temperatures rise due to climate change, humans are experiencing more frequent, prolonged, and intense heatwaves (Intergovernmental Panel on Climate Change (IPCC), 2019; Perkins-Kirkpatrick and Gibson, 2017). These extreme heat events pose significant challenges to human health, livability, productivity, and overall well-being (Ebi et al., 2021, 2020; Vanos et al., 2023). Vulnerable populations, such as the elderly, those with pre-existing medical conditions, and individuals living in poverty, are at heightened risk (Jay et al., 2021; Trenberth et al., 2003). Understanding the degree of heat strain associated with extreme heat across various demographics and activities is important for informing behavioral, policy, and infrastructure decisions aimed at mitigating these dangers (Cissé et al., 2022; Joshi et al., 2023a; Karanja et al., 2024; Vanos et al., 2024).

Heat strain assessment involves consideration of the energy balance of the human body and thermoregulatory processes. The energy balance includes heat generated internally (from metabolism and physical activity), heat and mass transfer pathways between the body and the environment (i.e., convection, radiation, and evaporation), and factors that affect these pathways. In particular, the degree of heat strain on human body is impacted by air temperature, ambient vapor pressure, air speed, long- and short-wave radiation (or mean radiant temperature), internal heat generation and redistribution within the body, and the thermal properties of clothing. Many human energy balance models and heat indices provide simplified representations of environmental stress, for example, only considering air temperature and humidity. In contrast, more advanced models incorporate complete treatment of environmental exposure with thermoregulatory controls driven by thermoreceptors, which sense the current thermal state of the body, either in the brain or in both the brain and skin(Stolwijk, 1971; J. A. J. Stolwijk and Hardy, 1966). Based on feedback from thermoreceptors, the hypothalamus activates thermoregulatory responses (such as vasomotion, sweating, and shivering) that aim to maintain the body's core temperature at healthy levels.

Advanced thermoregulatory models output comprehensive information about heat strain, such as core temperature, skin temperature, sweat rate, skin wettedness, cardiac output, and thermal comfort levels. Furthermore, advanced models can be extended to account for the effect of age, body mass index (BMI), gender, and other conditions that impact thermoregulatory functions to assess the heat strain at an individual level (Davoodi et al., 2018; Havenith, 2001, 1997; Takada et al., 2009; Takahashi et al., 2021; Van Marken Lichtenbelt et al., 2007; Zhang et al., 2001). Such tailoring can enable a nuanced understanding of how diverse populations are affected by complex environmental conditions, offering valuable insights for improving health and safety in extremely hot conditions (Deng et al., 2018; Karanja et al., 2024; Ou et al., 2023; Vanos et al., 2024; Zhao et al., 2020). However, uncertainty regarding the reliability and validation of models for heat exposure as well as availability (open source vs. commercial software that might be out of the financial reach of many researchers) are significant obstacles in analyzing the health risks posed by current and future heatwaves.

This study evaluated five thermoregulation models representing a wide range of complexity regarding thermoregulatory mechanisms, body segments, and tissue types (see Figure 1). The selected models include the two-node (single segment: core and skin) model by Gagge, two versions of the 25-node (six body segments) model by Stolwijk, 85-node JOS3 model (17 segments), and 187-node UTCI-Fiala multi-node model (12 segments) (Fiala et al., 2012; Gagge, 1971; Stolwijk, 1971; Takahashi et al., 2021). In addition, we introduce Stolwijk-2024 model, a modified version of the original model with updated empirical coefficients reflecting contemporary data from recent human trials while retaining the original framework. Besides the open-source models (either previously available or published with this paper), we also included results from the commercial UTCI-Fiala model because it is comprehensively validated and used in developing the Universal Thermal Climate Index (UTCI) that often serves as a benchmark (Jendritzky et al., 2012; Psikuta et al., 2012). We could not include recent complex 3D numerical models in the direct comparison, as the lack of published source code makes it challenging to reproduce them accurately (Castellani et al., 2021; Joshi et al., 2022; Kang et al., 2019; Nelson et al., 2009; Silva et al., 2018). Evaluating the selected five models using the same heat exposure and human trial data can reveal whether increased complexity improves accuracy in predicted physiological parameters and if simple, open-source models can perform reliably. To test the robustness and reliability of the models, we selected human subject data from the literature that covers a wide range of conditions for validation. These conditions include:

(i) extreme heat exposures where subjects transitioned between moderate and extreme conditions, reflecting transient air temperature and humidity,
(ii) hot and humid environments with high wet bulb temperatures,
(iii) scenarios where the mean radiant temperature is significantly higher than the air temperature,
(iv) various physical activities conducted in warm to hot conditions and
(v) a diverse range of clothing ensembles with differing levels of thermal insulation.

Evaluating these models will guide future developments and enable their use in public weather services, health systems, urban design, tourism, and climate impact research for accurate heat strain predictions.

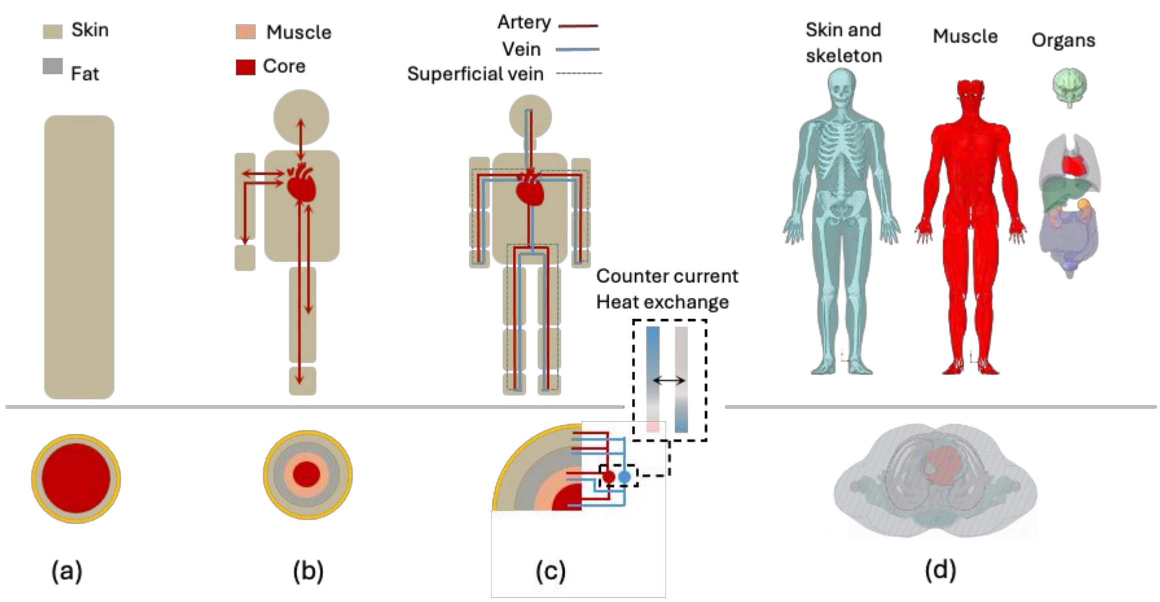

Figure 1. Side and cross-sectional overview of thermoregulation modeling approaches with varying levels of complexity; (a) single segment multi-node model (e.g., Gagge, 1971), (b) multi-segment multi-node model with simplified vascular system (e.g., Stolwijk, 1971), (c) multi-segment multi-node model with detailed vascular system (e.g., Fiala et al., 2012; Takahashi et al., 2021), and (d) 3D-anatomic thermoregulation models (e.g., Castellani et al., 2021; Nelson et al., 2009; Silva et al., 2018).

2. Methods

2.1 Overview and rationale for the five model selection

Since the 1960s, mathematical models of human thermoregulation have evolved in complexity, incorporating factors like thermal physiology, body geometry, clothing, and environmental influences on heat transfer (Castellani et al., 2021; Fiala et al., 2012; Gagge, 1971; Joshi et al., 2022; Kang et al., 2019; Nelson et al., 2009; Silva et al., 2018; Stolwijk, 1971; Takahashi et al., 2021; Tanabe et al., 2002; Wissler, 2018). Among these, the Gagge model (Gagge, 1971) consists of a single segment with two nodes representing the core and skin. In this model, the thermal properties of different tissues are lumped together within these two nodes. Because the model is limited to a single segment, it has a restrictive capacity for capturing variations in key thermoregulatory mechanisms, such as heat generation, blood flow, and sweating, which differ significantly across various body segments. These limitations constrain the model's ability to calculate these mechanisms with higher spatial resolution. Despite this limitation, it has been used as heat strain and thermal comfort assessment tool due to its simplicity and accuracy (Haslam and Parsons, 1994, 1988; Ooka et al., 2010; Standard, 1992; Tartarini et al., 2020).

The Stolwijk-1971 model includes six body segments and four tissue types (core, muscle, fat, and skin) allowing for detailed spatial resolution in thermoregulatory analysis, as described in described in Figure 1b (Stolwijk, 1971). The multi-segmented nature of the model enables the detailed definition of thermal properties for body tissues and clothing layers in individual segments, allowing for higher spatial resolution in representing thermoregulatory mechanisms. Stolwijk's and similar models assume that each node directly exchanges heat with a central blood pool. It is also critical to point out that validation of Stolwijk-1971 model and its derivatives have generally been limited to low activity levels under semi-nude conditions (Munir et al., 2009; Roelofsen et al., 2023; Roelofsen and Vink, 2016; Stolwijk, 1971; Tang et al., 2020). In the Stolwijk-2024 model, we updated the Stolwijk-1971 thermoregulation model by incorporating recent findings, including updated weighing factors for various thermoregulatory mechanisms, heat transfer coefficients, and improved methods for calculating heat transfer through clothing, as described in the Supplemental Material (SM).

The Stolwijk model has served as foundation for many existing thermoregulation models, with its derivative models enhancing the original model (referred as Stolwijk-1971) by improving thermoregulatory systems, body segmentation, and individual characteristics of thermoregulations (Huizenga et al., 2001; Roelofsen and Vink, 2016; Stolwijk, 1971; Takada et al., 2009; Takahashi et al., 2021; Tanabe et al., 2002; Tang et al., 2020; Zhang et al., 2001), and detailed heat transfer through arteries and veins (Dongmei et al., 2012; Ooka et al., 2010; Takada et al., 2009; Takahashi et al., 2021). More recent developments in thermoregulation models significantly improve the spatial resolution by increasing the number of body segments and, consequently, the number of nodes (Fiala et al., 2012; Takahashi et al., 2021). Furthermore, these models also consider the improved thermoregulatory mechanisms, especially heat transfer via blood flow through the complex networks of arteries and veins (Fiala et al., 2012; Takahashi et al., 2021). The JOS-3 and UTCI-Fiala models consider the counter-current heat exchange and convective heat transfer in capillary beds and local tissue. Therefore, arteries at each segment have different blood temperatures, leading to potentially large differences for extremities (e.g. hand and feet) due to convective heat transfer in upstream segments. Such characteristics are particularly important in cold temperatures and cannot be captured by the Stolwijk model where all the segments exchange heat with the central blood pool that is at one particular thermal state at any given time (Fiala et al., 2012; Gagge, 1971; Stolwijk, 1971;

Takahashi et al., 2021). The key features and rationale for model selection for comparison are also summarized in Table 1.

Table 1. Key features and rationale for the model selection

Model and year	Number of body segments	Number of nodes	Key features
Two-node Gagge (1971)	1	2	Widely used model for assessing heat strain and thermal comfort due to its simplicity.
Stolwijk (1971)	6	25	Serves as the foundation for many modern thermoregulation models. Uses simplified blood flow, where each node exchanges heat directly with a central blood pool.
Modified Stolwijk (2024)	6	25	Updated version of the Stolwijk-1971 model, incorporating recent advancements in vasomotion control, shivering, sweating, heat transfer coefficients, and heat transfer through clothing.
JOS-3 (2021)	17	85	Models counter-current heat exchange in arteries and veins, along with convective heat transfer in capillaries and local tissues,
UTCI-Fiala (2012)	12	187	The foundation model for the Universal Thermal Climate Index (UTCI), validated for assessing heat strain across a wide range of environmental conditions. Similar to JOS-3, models major key thermoregulatory mechanisms.

2.2. Improved thermoregulation model: Stolwijk-2024

The improved Stolwijk-2024 thermoregulation model consists of six body segments: head, trunk, arms, hands, legs, and feet. Each segment includes four concentric layers (core, muscle, fat, and skin) along with a node representing the central blood compartment (Figure 1(b)). This section focuses on the modifications made primarily to the control system to enhance the accuracy and functionality of the classical Stolwijk model. Additionally, the set point temperatures for each node and the heat exchange with the environment through clothing were updated in the new Stolwijk-2024 model. For a detailed description, please refer to the supplemental material.

The control system of human thermoregulation receives signals from thermoreceptors and processes them in the hypothalamus. Based on these signals, the control system activates various thermoregulatory mechanisms such as vasoconstriction, vasodilation, shivering, and sweating. Stolwijk (Stolwijk, 1971) defined the control system based on error signals defined as the difference between actual temperature at any given time and set point temperature at given node (see Equations 1 to 5). Accordingly, a positive error signal indicates warm sensing at the thermoreceptors, while a negative error signal indicates cold sensing. The mathematical form of the thermoregulatory mechanisms considers signals from both central and skin thermoreceptors.

$$ERR_{j,i} = T_{j,i} - T_{set_{j,i}} \tag{1}$$

$$WRM_{j,i} = max(ERR_{j,i}, 0) \quad (2)$$
$$CLD_{j,i} = |min(ERR_{j,i}, 0)| \quad (3)$$
$$WRMS = \sum_{j=0}^{5} D\,F_{TR_j} \cdot WRM_j \quad (4)$$
$$CLDS = \sum_{j=0}^{5} D\,F_{TR_j} \cdot CLD_j \quad (5)$$

where, ERR is error signal $(°\mathrm{C})$, $\mathrm{T_{j,i}}$ is temperature of given node and body segment $(°\mathrm{C})$, $\mathrm{T_{set_{j,i}}}$ is set point temperature (temperature at physiological thermal neutrality) of given node and body segment $(°\mathrm{C})$, $\mathrm{WRM_{j,i}}$ is warm sensing signal $(\mathrm{N.D.})$, $\mathrm{CLD_{j,i}}$ is cold sensing signal $(\mathrm{N.D.})$, WRMS is total warm thermoreceptors signal $(\mathrm{N.D.})$, CLDS is total cold thermoreceptors signal $(\mathrm{N.D.})$, and $\mathrm{DF_{TR_j}}$ is distribution of thermoreceptor over different body segments $(\mathrm{N.D.})$

Stolwijk assumed that effector part of thermoregulation system can be modelled by the control equations, which combine weighted signal from hypothalamus (central thermoreceptor), and integrated signal from the skin thermoreceptors (Stolwijk, 1971). Based on these assumptions Stolwijk suggested the controller equations for various thermoregulatory mechanisms, as described in Equations 6 to 9 (Stolwijk, 1971). Recently, the JOS-3 thermoregulation model proposed updated control coefficients (Takahashi et al., 2021), which are incorporated into the present study. These control coefficients have significant impact on efferent signals such as vasomotion, sweating, and shivering. As shown in Figure 2, simulation follows a 240-minute transient exposure, structured as 60 minutes in a moderately cool environment at 28°C, 120 minutes in an extreme heat condition at 47.8°C, and a final 60 minutes back at 28°C (Case 7 in Table 2). Figure 2a illustrates the responses of afferent signals from skin and central thermoreceptors, which trigger various efferent thermoregulatory actions in both the original Stolwijk-1971 model and the modified Stolwijk-2024 model (Figure 2b to 2e).

$$SW = (371.2 \cdot ERR_{Head_{core}}) + (33.64 \cdot (WRMS - CLDS)) \quad (6)$$
$$VD = (100.5 \cdot ERR_{Head_{core}}) + (6.4 \cdot (WRMS - CLDS)) \quad (7)$$
$$SH = 24.36 \cdot ERR_{Head_{core}} \cdot CLDS \quad (8)$$
$$VC = (-10.8 \cdot ERR_{Head_{core}}) + (-10.8 \cdot (WRMS - CLDS)) \quad (9)$$

where, SW is total efferent sweat signal (W), $\mathrm{ERR_{Head_{core}}}$ is error signal from central thermoreceptor, representing changes in hypothalamus $(\mathrm{N.D.})$, VD is total efferent skin vasodilation signal $(\mathrm{N.D.})$, SH is total efferent shivering signal (W), VC is total efferent skin vasoconstriction signal $(\mathrm{N.D.})$

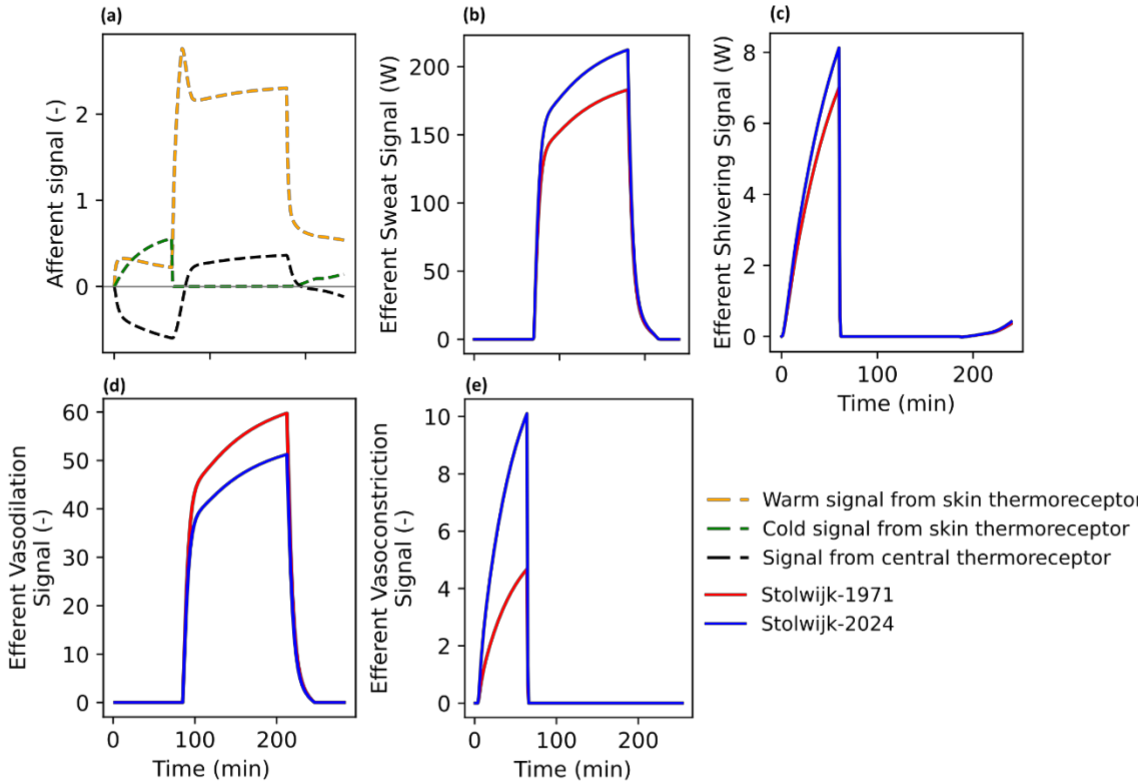

Figure 2. (a) Afferent signals from various thermoreceptor; Comparison of efferent signal from Stolwijk-1971 and improved Stolwijk-2024 model for given afferent signals (b)efferent sweating signal, (c) efferent shivering signal, (d) efferent vasodilation signal, and (e) efferent vasoconstriction signal.

2.3. The human trial cases used for evaluating performance of the models

The five selected models with varying level of complexity were evaluated to predict core and mean skin temperature across a wide range of parameters affecting the body's heat balance. The models were evaluated under a wide range of conditions, including air temperature, mean radiant temperature, relative humidity, air speed, activity levels, and clothing thermal insulation, as detailed in **Table 2**. The validation cases were focused on moderate to extreme hot climatic conditions (T_{air}: 21 to 49.5°C, MRT: 21 to 57°C, RH: 21 to 69.4 %, and v_{air}: 0.1 to 3.3 $m \cdot s^{-1}$ along with various metabolic activity levels (0.8 to 12.1 met) and clothing insulation (0.016 to 0.262 $m^2 \cdot K^{-1} °C^{-1}$)). The thermal and evaporative resistances presented in Table 2 are obtained from reported values in respective literature of human trial data and based on clothing descriptions especially for nude or semi-nude conditions. The accuracy and precision of the predicted core and skin temperatures were assessed using the root-mean-square deviation (RMSD) and bias. The UTCI-Fiala model was evaluated in 9 out of the 15 heat exposure cases (Table 2), where both simulated core and/or skin temperature data were available from the literature. Due to licensing restrictions, the UTCI-Fiala model could not be applied to the remaining cases. In cases 10 to 15, only core temperature data were reported in literature, so comparisons were made exclusively for core temperatures, as skin temperature data were not available.

$$\mathrm{RMSD} = \sqrt{\frac{\sum_{i=1}^{n}(x_i - \hat{x}_i)^2}{n}} \quad (1)$$

$$\mathrm{Bias} = \frac{\sum_{i=1}^{n}(x_i - \hat{x}_i)}{n} \quad (2)$$

where, RMSD is root-mean-square deviation of the thermoregulation model, Bias is bias of the thermoregulation model, i is data point in given time series, n is total number of data points in given time series, x_i = experimental data points, and $\hat{x}_i$ = simulated data points. A model's predictive performance is considered acceptable when the RMSD falls within the maximum standard deviation of core temperature (0.5°C) and mean skin temperature (1.6°C), based on experimental data from 590 human subject experiments across 80 different ambient conditions (Haslam and Parsons, 1994; Joshi et al., 2022).

Table 2. Details of environmental conditions, activity level, and clothing resistance for comparison of the thermoregulation models.

Case	Duration [min]	T_{air} [°C]	MRT [°C]	RH_{air} [%]	V_{air} [$m \cdot s^{-1}$]	Metabolic rate [met]	R_{cl} [$m^2 \cdot °C^{-1} W^{-1}$]	R_{ecl} [$m^2 \cdot Pa^{-1} W^{-1}$]	Source
Case 1	130	30	30	30	0.1	1.0 to 3.6	0.016	2.5	(Haslam and Parsons, 1988; Psikuta et al., 2012)
Case 2	240	27.8 to 33.3	27.8 to 33.3	37 to 34	0.1	0.8	0	0.0	(Stolwijk and Hardy, 1966a)
Case 3	240	28.5 to 37.5	28.5 to 37.5	41 to 33	0.1	0.8	0	0.0	(Stolwijk and Hardy, 1966a)
Case 4	400	21 to 39.6	21 to 39.6	40 to 69	0.2	1 to 3.0	0.040	7.0	(Smallcombe et al., 2022)
Case 5	180	28 to 45	28 to 45	53 to 21	0.1	1.1 to 2.4	0.016	2.5	(Psikuta et al., 2012)
Case 6	240	28 to 42.5	28 to 42.5	37 to 28	0.1	0.8	0	0	(Stolwijk and Hardy, 1966a)
Case 7	240	28.1 to 47.8	28.1 to 47.8	43 to 27	0.1	0.8	0	0	(Stolwijk and Hardy, 1966a)
Case 8	90	43	43	57	0.15	1.6	0.078	6.0	(Song et al., 2019)
Case 9	160	28 to 36	28 to 57	25 to 15	0.5	1.8 to 3.9	0.016 to 0.093	2.5 to 14.8	(Psikuta et al., 2012)
Case 10	40	28	28	50	3.28	12.1	0.016	2.5	(Jack, 2009; Psikuta et al., 2012)
Case 11	40	28	28	50	3.28	9.2	0.016	2.5	(Jack, 2009; Psikuta et al., 2012)
Case 12	90	49.5	49.5	32	0.1	1.0 to 4.4	0.016	2.5	(Haslam and Parsons, 1988; Psikuta et al., 2012)
Case 13	120	40	40	40	0.2	3.4	0.016	2.5	(Moran et al., 1998; Psikuta et al., 2012)
Case 14	100	35	35	50	1	4.0	0.127	20.3	(Gonzalez et al., 1997; Psikuta et al., 2012)
Case 15	100	35	35	50	1	3.8	0.262	41.8	(Gonzalez et al., 1997; Psikuta et al., 2012)

3. Results

The simulation results cover a broad spectrum of environmental and physical activity conditions, providing insights into the predictive performance of thermoregulation models with varying levels of complexity. These models were tested under scenarios including transient and extreme dry-heat exposures, humid-heat environments, high radiative heat sources, and different levels of physical activity in moderate to hot climates. The validation process also included cases with varying degrees of clothing insulation and physical activity levels to ensure a comprehensive model evaluation. The following subsections evaluate the performance of the models in specific scenarios.

3.1 Transient exposure to moderate climate (Cases 1-4)

Prior to the application of thermoregulation models in extreme climates, we assessed their performance in scenarios with moderate to low heat strain (Figure 3, Cases 1-4). Although the risk of heat illness in these cases is low, the predicted core and skin temperatures are useful indicators of thermal comfort and sensation.

In Case 1, where 11 male subjects exercised in a moderate environment (Haslam and Parsons, 1988; Psikuta et al., 2012), most thermoregulation models accurately predicted the increase in both core and skin temperatures (Figure 3). However, the UTCI-Fiala model consistently underpredicted skin temperature throughout the exposure, with an RMSD of 1.6°C. Psikuta et al. (Psikuta et al., 2012) observed similar underprediction in other cases with higher activity levels, possibly due to impaired sweat evaporation at the measurement site, where the skin temperature sensor was taped using semi-permeable tape. Despite this, the other models we evaluated accurately predicted the magnitude and trend of skin temperature.

In Cases 2 and 3, three subjects were exposed to transient, moderately warm environments (Stolwijk and Hardy, 1966b), alternating between chambers with different air temperatures, as shown in Figure 3. All models predicted core and skin temperatures with acceptable accuracy for these exposures. However, in models with a simplified vascular and blood flow system (such as Gagge's two-node model and both Stolwijk models), the predicted core temperature responded more quickly to changes in air temperature. In contrast, models with a more detailed vascular system (like JOS-3 and UTCI-Fiala) showed a slower response, with trends that better aligned with those observed in human subjects.

Case 4 involved highly transient environmental conditions and activities, where the human subject followed a work-rest cycle typical of occupational workers, alternating between a warm environment (39.6°C) and a comfortable environment (21°C) (Smallcombe et al., 2022). All models satisfactorily predicted core and skin temperatures within acceptable thresholds (Figure 3), except for Gagge's two-node model, which showed an RMSD of 0.68°C above the acceptable range for predicted core temperature.

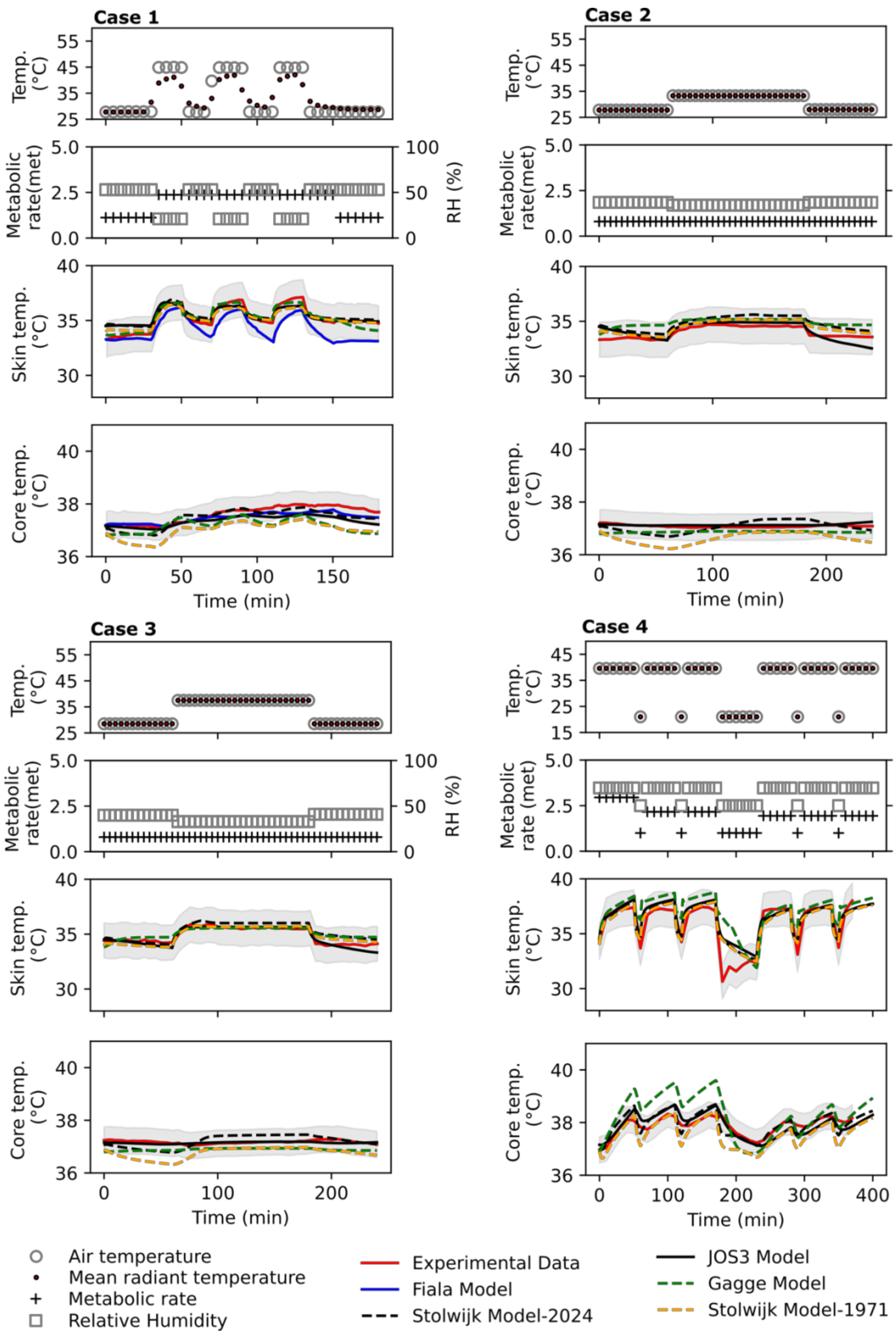

Figure 3. Evaluation of thermoregulation model for moderate to warm exposure (Cases 1 to 4, Table1); Shaded area represents the deviation in measured data.

3.2 Transient and extreme dry-heat exposure (Cases 5-7)

In Cases 5 to 7 (Table 2), air temperature, mean radiant temperature, and relative humidity varied from moderate to extreme heat conditions, while activity levels remained constant with nude or semi-nude subjects. In Case 5, six human subjects exercised at a constant metabolic rate (2.4 met) while air and mean radiant temperature alternated between 28°C and 45°C (Psikuta et al., 2012). The Stolwijk-1971 and Gagge two-node models significantly underpredicted core temperature by 0.63°C and 0.53°C, respectively. The UTCI-Fiala model underpredicted skin temperature by 1.2°C. In contrast, the other models accurately predicted both the trend and absolute values of core and skin temperatures (Figure 4).

In Cases 6 and 7, three subjects were exposed to alternating air temperatures and relative humidity (Stolwijk and Hardy, 1966a). The predicted core and skin temperatures were within the acceptable range for all models, except for the Stolwijk-1971 model in Case 7, where the RMSD for predicted core temperature (0.67°C) exceeded the acceptable range of 0.5°C. In contrast, the Stolwijk-2024 model demonstrated a lower RMSD (0.35°C) in predicted core temperature, highlighting the importance of incorporating updated set-point temperatures, heat transfer coefficients, and other thermoregulatory coefficients in improving model accuracy.

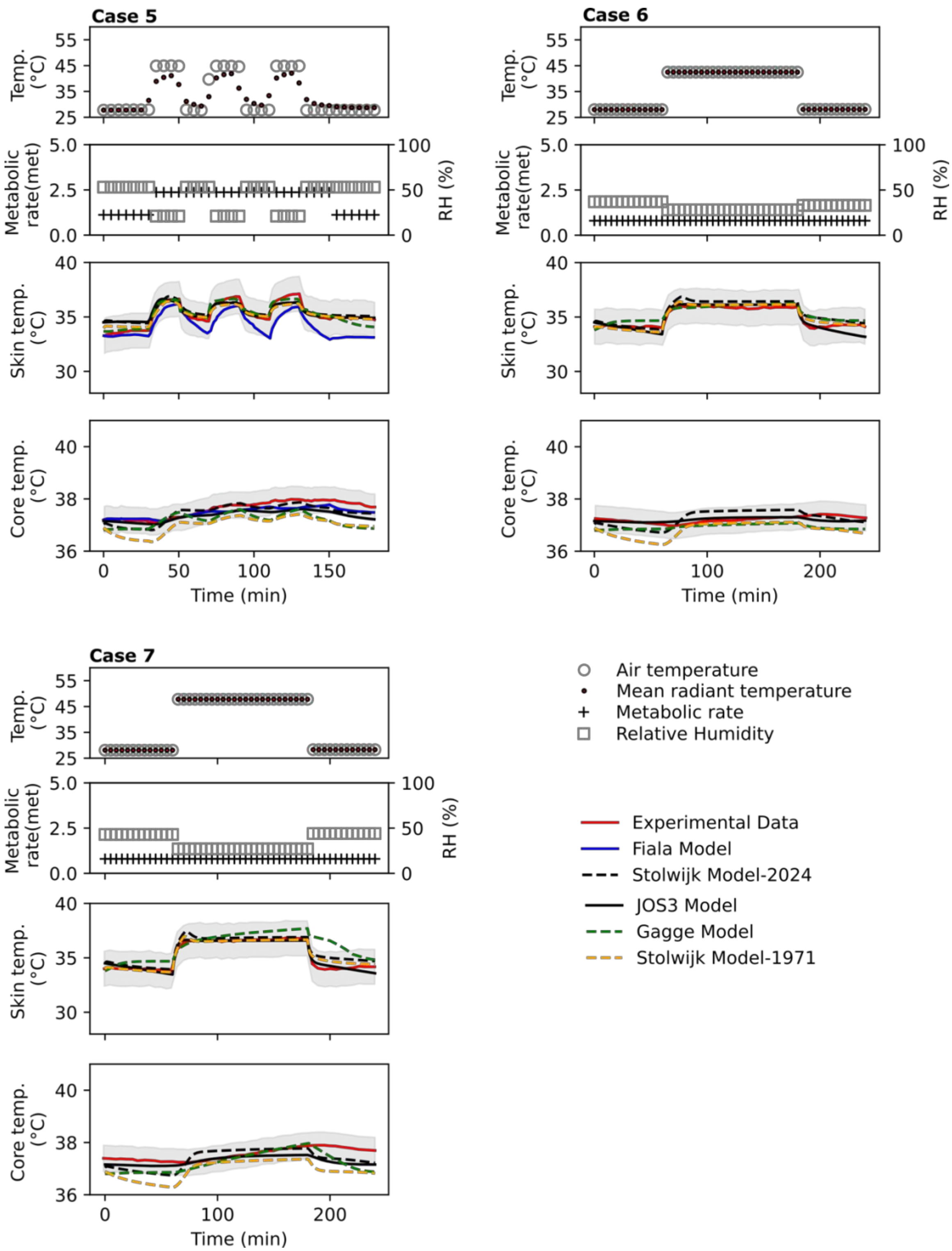

Figure 4. Evaluation of thermoregulation models for extreme dry-heat exposures (Case 5 to 7 in Table 2); Shaded area represents the deviation in measured data.

3.3 Humid-heat exposure (Case 8)

In Case 8, human subjects were exposed to hot (43°C) and humid (57% RH) conditions, with a wet bulb temperature of 34.2°C, for 90 minutes (Song et al., 2019). All models accurately predicted the simulated core and mean skin temperatures, showing good agreement with the measured experimental data (Figure 5). During the first 20 minutes of exposure, the core temperature rose slowly, indicating increased strain on the thermoregulatory system. As the exposure continued, both core and skin temperatures steadily increased, suggesting that autonomic thermoregulation, including vasodilation and sweating, was insufficient to maintain core temperature at safe levels.

3.4 Intense radiative exposure (Case 9)

Another common scenario in extreme heat conditions involves intense exposure to short- and long-wave radiation, which can be expressed as high mean radiant temperatures. To evaluate the models under such conditions, we modeled Case 9 in which five semi-nude ($0.016\ m^2 \cdot °C^{-1} W^{-1}$) human subjects were exposed to a radiant heat source positioned in front of them. In all models we simulated the radiant heat fluxes as mean radiant temperature (Psikuta et al., 2012). At the 80-minute mark, the subjects donned light clothing ($0.093\ m^2 \cdot °C^{-1} W^{-1}$), leading to a significant deviation in core temperature values predicted by the two-node Gagge model. All other models accurately predicted both core and mean skin temperatures within acceptable thresholds (Figure 5). The significantly higher radiant temperature of 57°C caused elevated core and skin temperatures, indicating heat strain; however, thermoregulatory mechanisms such as sweating and vasodilation were able to compensate for the excess heat, maintaining core temperature below the dangerous levels associated with heat stroke or exhaustion.

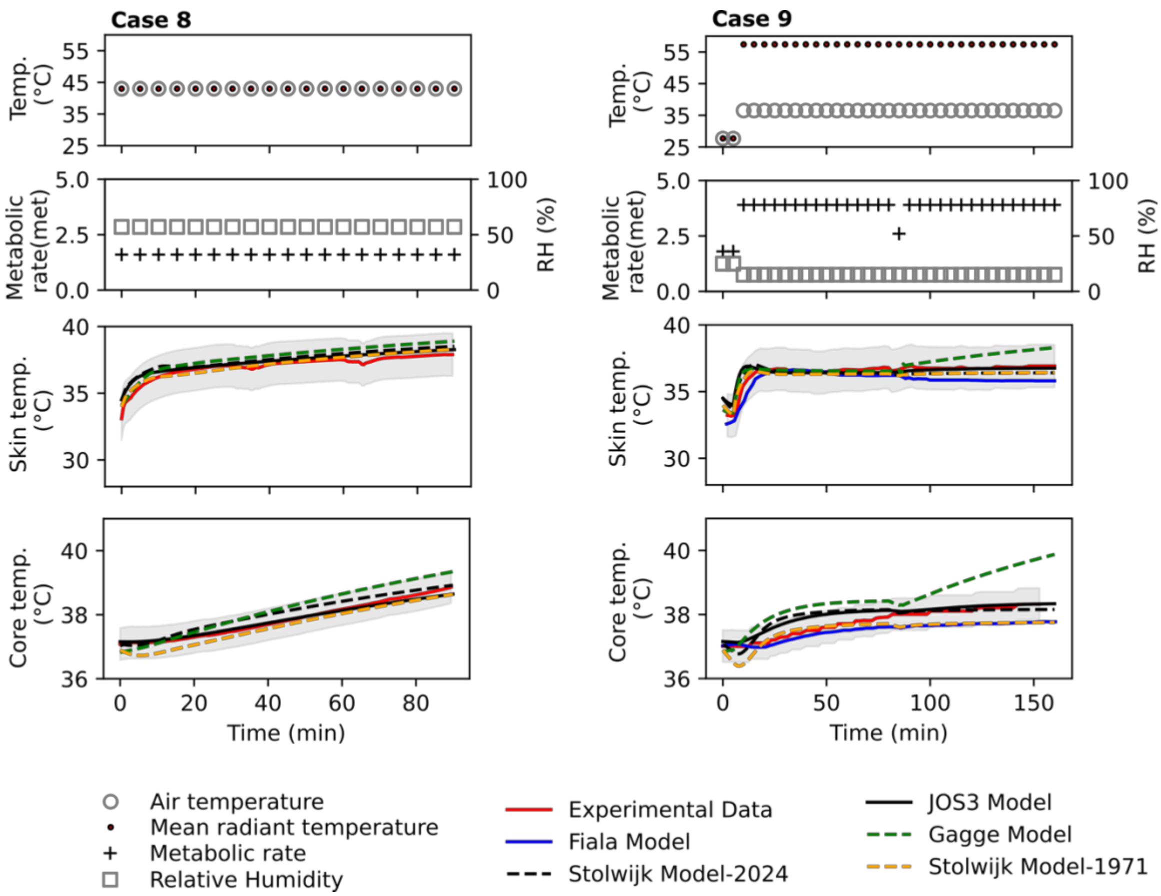

Figure 5. Evaluation of models for hot and humid conditions (43°C and 57%RH, representing the high wet bulb temperature of 34.2°C) and high mean radiant temperature (57°C) exposures (Cases 8 and 9 in Table 2); Shaded area represents the deviation in measured data.

3.5 Varied physical activity levels in moderate to hot climate (Cases 10-15)

To address the conditions of occupational workers and athletes with various level of clothing thermal insulation and physical activities, cases 10 to 15 (Table 2) were evaluated for intense physical activities (ranging from 3.35 to 12.1 met) and high clothing thermal (0.262 $m^2 \cdot °C^{-1}W^{-1}$) and evaporative (41.8 $m^2 \cdot °C^{-1}W^{-1}$) resistances (Gonzalez et al., 1997; Haslam and Parsons, 1988; Jack, 2009; Moran et al., 1998; Psikuta et al., 2012). The predictive ability of the models for the skin temperature could not be tested for these cases, as it was not available in literature.

In case 10, professional athletes ran on treadmill at moderate ambient temperatures and very high metabolic rate of 12.1 met (Jack, 2009; Psikuta et al., 2012). For this case, UTCI-Fiala and two-node model significantly overpredicted the core temperature (RMSD: 0.9 and 1.2 °C). On the other hand, Stolwijk-1971 model underpredicted the core temperature by 0.72 °C. These discrepancies in predicted core temperature potentially emerge from the limitations of the sweat and vasodilation controls in the original model. The JOS-3 and Stolwijk-2024 model accurately predicted the core temperature of intense activity levels. Case 11 is similar to case 10, where activity was performed by recreational athletes, hence at lower metabolic rate of 9.2 met compared to professional athletes. For, case 11 all the models accurately predicted the core temperature.

For case 12, five human subjects were exposed to extreme heat conditions (49.5 °C) for 90 mins, where for first 45 min metabolic activity was 1.0 met and for later 45 mins at 4.42 met (Haslam and Parsons, 1988; Psikuta et al., 2012). For this exposure, JOS-3, Stolwijk-2024, and two-node model overpredicts (0.6, 0.8, and 1.2 °C, respectively) the core temperature beyond the acceptable limit; while the UTCI-Fiala and Stolwijk-1971 model predicts the core temperature accurately (Figure 6).

In case 13, 100 human subjects were exposed to hot and humid environment (40 °C 40% RH) with moderate physical activity at 3.35 met. For this scenario, the core temperature predicted by all the models were in the acceptable range (Figure 6).

For Case 14 and 15, ten human subjects were exposed to moderately hot environments (35 °C, 50%RH) and performed physical activity at around 4 met. In Case 14 subjects were wearing clothing with thermal insulation of 0.127 $m^2 \cdot °C^{-1} W^{-1}$, while in case 15 subjects were wearing a more thermally insulative clothing at 0.262 $m^2 \cdot °C^{-1} W^{-1}$. For these cases with varying level of clothing thermal insulation, all models accurately predicted the core temperature except the Gagge’s two-node model (Figure 7).

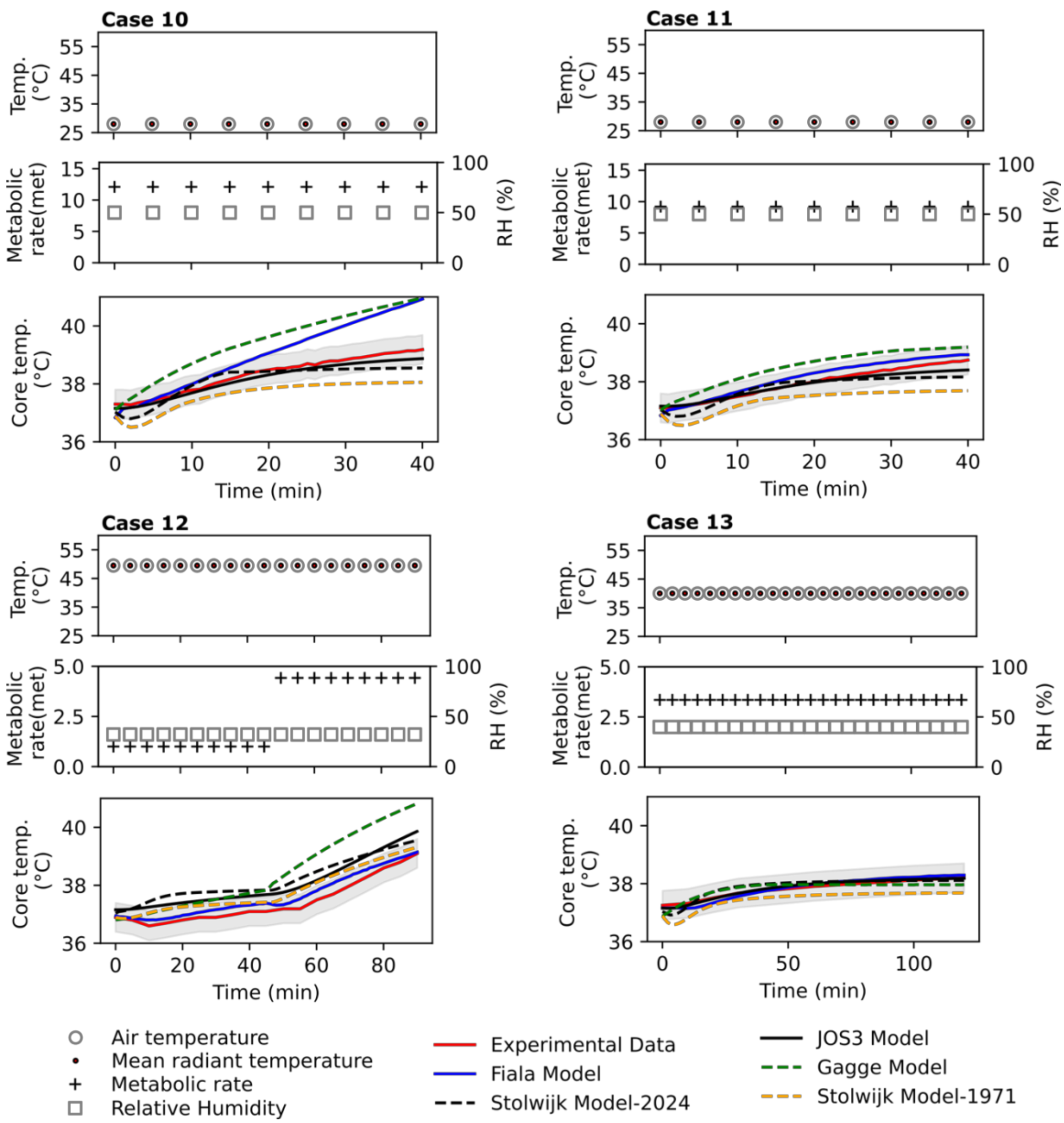

Figure 6. Evaluation of the models for wide range of physical activities (1.0 to 12.1 met) under moderate to extreme heat environment (Cases 10 to 13 in Table 2); Shaded area represents the deviation in measured data.

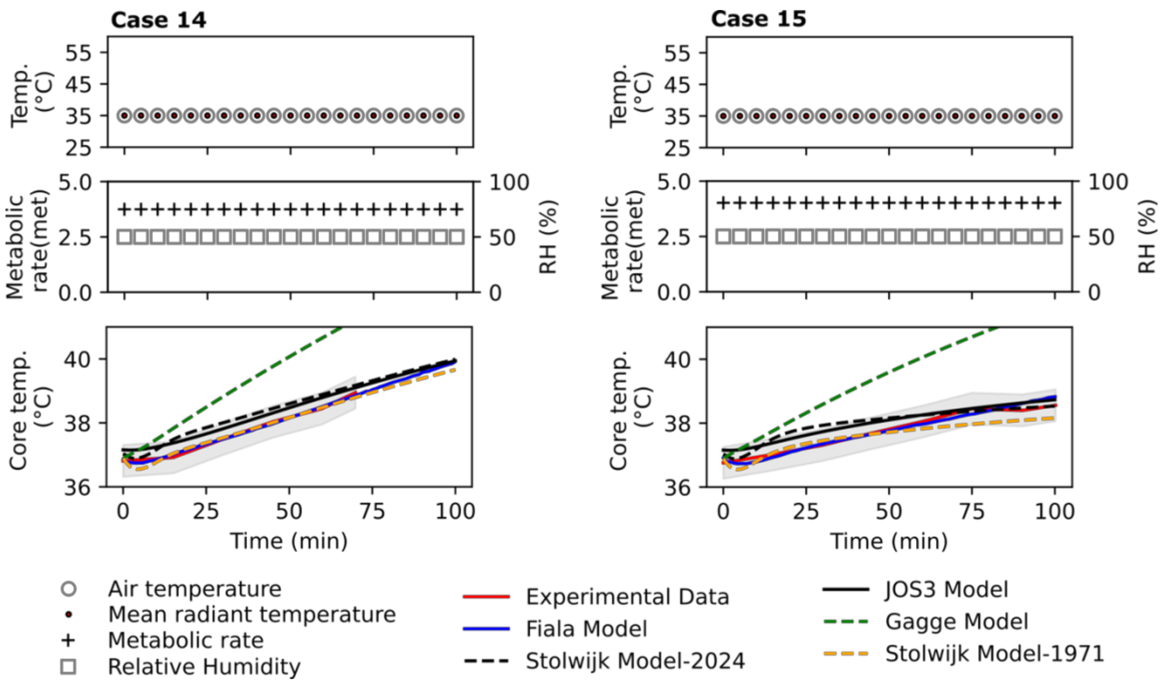

Figure 7. Evaluation of the models for different level of clothing thermal insulation (0.127 and 0.262 $m^2 \cdot K^{-1} W^{-1}$) (Cases 14 and 15 in Table 2); Shaded area represents the deviation in measured data.

4. Discussion

4.1 Evaluating model performance in predicting the core and skin temperatures

The predictive accuracy of core and mean skin temperatures was evaluated using Root Mean Square Deviation (RMSD) and Bias (Figure 8), revealing that most models performed well within acceptable thresholds across these diverse validation scenarios (Table 2). However, the two-node Gagge's model and the Stolwijk-1971 model with legacy coefficients, exhibited limitations under specific conditions, such as extreme heat, high physical activity, or highly transient environments, where deviations from the experimental data on human subjects were observed. Multi-segment models (JOS3, UTCI-Fiala, and Stolwijk-2024) demonstrated strong predictive performance for core temperature, with average RMSD values across all cases of 0.22 ± 0.15°C, 0.25 ± 0.26°C, and 0.31 ± 0.16°C, respectively. These values fall within the acceptable range of the maximum standard deviation (0.5°C) observed in measured core temperatures from human subjects (Haslam and Parsons, 1994; Joshi et al., 2022). As shown in Figure 8, each of these multi-node models had one outlier where the RMSD of predicted core temperature exceeded 0.5°C. For the JOS3 and Stolwijk-2024 models, this occurred under conditions of very high ambient temperature (49.5°C, Case 12), while the Fiala model showed lower accuracy for cases involving very high metabolic rates (12.1 met, Case 10). The bias in predicted core temperature for these three models was close to zero -0.04°C, -0.08°C, and -0.09°C, respectively indicating very good accuracy. Overall, these multi-node models performed well across a wide range of conditions, including exposure to dry heat, humid heat, various levels of physical activity, and different clothing thermal properties.

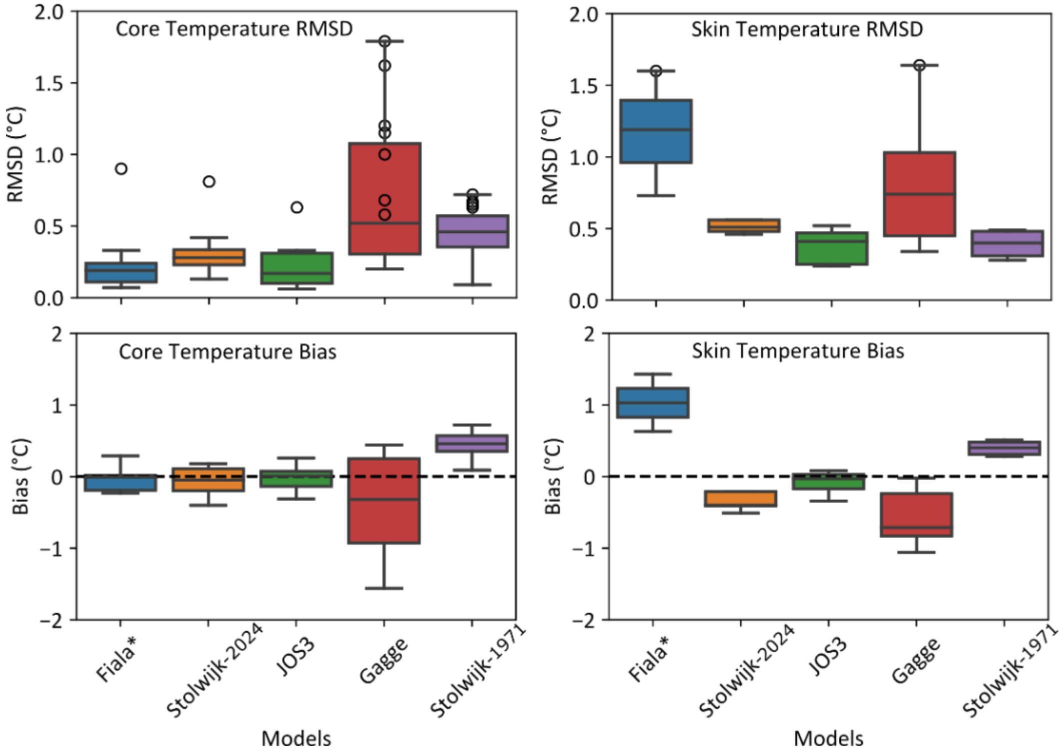

Figure 8. Root-mean-square deviation (RMSD) and bias of simulated core and mean skin temperature, Outlier marker represents the cases where simulated values of temperature were beyond the acceptable range (0.5°C for core and 1.6°C for mean skin temperature (Haslam and Parsons, 1988; Joshi et al., 2022)), *: Fiala's model validated for 9 cases only.

Comparing the predicted values from models to human subject data for the same heat exposure offers a clearer understanding of the strengths and limitations of each model. The original Stolwijk model (Stolwijk-1971) and the Gagge's model exhibited relatively high RMSD values in predicting core temperature, with 0.45 ± 0.18°C and 0.71 ± 0.52°C, respectively. Both the Stolwijk-1971 and Gagge's two-node models performed poorly in cases involving high metabolic rates and hot exposures. Specifically, the Stolwijk-1971 model consistently underpredicted core temperatures in cases with high metabolic rates (cases 10 and 11). This model also demonstrated a positive bias of 0.45 °C (Figure 8) in predicted core temperature, indicating a systematic underprediction. One possible reason for this underprediction could be the setpoint temperature of the hypothalamus (Table S1 to S3 in SM) and the coefficients used in the thermoregulatory control system (equations S7 to S10 in SM). When comparing the setpoint temperatures of the Stolwijk-1971 model with those of the JOS-3 (or Stolwijk-2024) models, it becomes evident that the setpoint temperatures in the Stolwijk-1971 model are significantly lower (by up to 0.5°C). This lower setpoint triggers an earlier onset of sweating and vasodilation, with higher magnitudes, leading to a reduction in core temperature. In contrast, the modified Stolwijk-2024 model shows significant improvement in predicting core temperature compared to the original Stolwijk-1971 model. This improved performance can be attributed to the updated setpoint temperatures (Table S1 in SM) and improved convective and radiative heat transfer coefficients (Table S3 in SM). On the other hand, although Gagge's two-node model did not exhibit a clear bias in predicted core temperature, its overall accuracy was lower in cases involving higher metabolic rates. This is likely because the model is a single-segment, two-node (core and skin) model, which oversimplifies the distribution of heat generated by physical activity. In reality, heat is distributed differently within the muscle layer of the body, a factor that cannot be effectively accounted for in such an oversimplified model.

Overall, in hot-dry conditions, there was a higher scatter and disagreement among different models. However, all models showed good agreement with measured core temperatures from human subjects during hot and humid exposures. This variation can be attributed to the differences in how each model handles sweating. As shown in Figure 9, various thermoregulation models have significant variations in efferent signals related to sweating due to underlying control coefficients and error signal (equations 1 to 9). Figure 9 represents the variation in sweat signal for two cases (case 7 and 10), where sweating signal expected to be the significant due to high heat strain due to environmental stress and physical activity. In dry conditions, the sweat rate becomes the driving factor, and the coefficients used by each model to simulate sweating vary significantly, leading to discrepancies in their performance. In contrast, during hot and humid exposures, the driving factor is sweat evaporation. Here, all models accurately predicted sweat evaporation, suggesting that the Lewis coefficient, which governs this process, is well established and effective across different models.

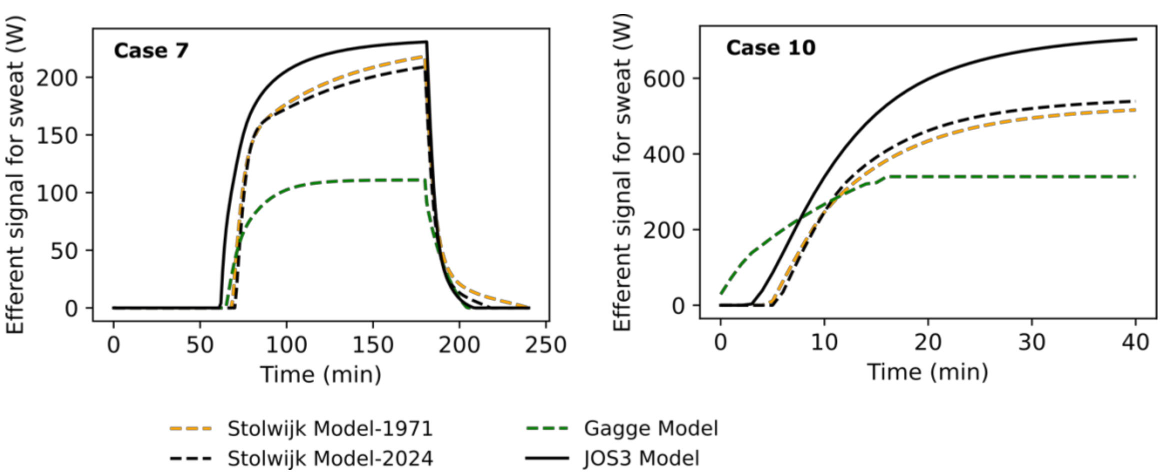

Figure 9. Efferent signal for sweating from active/control system of various thermoregulation models.

All the models predicted skin temperature with acceptable accuracy (RMSD < 1.6°C). The JOS3 and Stolwijk-2024 models consistently predicted mean skin temperature with low RMSD values (0.44°C and 0.56°C, respectively) and biases (-0.11°C and -0.30°C); both of which are significantly below the maximum standard deviation (1.6°C).

4.2 Model performance in relation to complexity and accessibility

Results from the validation study indicate that multi-node and multi-segment models, such as JOS-3, Stolwijk-2024, and UTCI-Fiala, excel because they define key thermoregulatory mechanisms, such as vasodilation, skin blood flow, and sweating, with higher spatial resolution. Notably, the JOS3 and UTCI-Fiala models offer detailed considerations of heat distribution due to blood flow, including counter-current heat exchange, to account for heat transfer through the network of arteries, veins, and superficial veins in the human body. In contrast, the Stolwijk-2024 model simplifies the process by assuming that each node exchanges heat with the central blood node through blood flow, which reduces model complexity. This simplification results in a marginally higher RMSD in core temperature when evaluated for various heat exposures, ranging from 0.06 to 0.09°C. However, the accuracy of the predicted skin temperature in the Stolwijk-2024 model remains comparable to more complex models like JOS-3 and UTCI-Fiala model. Therefore, the modified Stolwijk-2024 model is well-suited for analyzing heat strain and thermal comfort in moderate to extreme-hot environmental conditions. The simplification of heat transfer through blood flow is appropriate for heat strain assessment, as the spatial variation of temperature between different body segments and tissues is minimal due to high blood perfusion (Gordon et al., 1976; Haslam and Parsons, 1994). However, it is important to note that these findings cannot be extrapolated to cold-strain scenarios, where variation in skin blood flow and local skin temperature is significantly higher.

The validation of the thermoregulation models clearly highlights that multi-node and multi-segment models can effectively simulate and analyze physiological heat strain across a wide range of climatic conditions. Furthermore, open-source thermoregulation models, such as JOS3 and Stolwijk-2024, either already incorporate or can be relatively easily extended to account for factors that impact thermoregulatory functions, such as aging, acclimatization, body size, gender, hydration status, and medical conditions. In contrast, models like the UTCI-Fiala, which are integrated into commercial software requiring licenses, may present accessibility challenges for those without access to licensed software or resources. Such limitations make it cumbersome to reproduce, modify, or extend commercial models to account for specific conditions that impact thermoregulatory functions. Therefore, despite their comparable accuracy to open-source models, the complexity and limitations of many models from literature can pose significant challenges in their applications.

4.3 Limitations

The validation and comparison of the models in this study focused on analyzing heat strain in individuals corresponding to young, healthy, and averages of the population. However, this study did not account for inter-individual differences in thermoregulatory responses due to factors such as age, gender, and body composition (Kaciuba-Uscilko and Grucza, 2001; Matsumoto et al., 1999; Van Marken Lichtenbelt et al., 2007; Van Someren et al., 2002). These differences can significantly impact thermoregulatory functions and temperature distribution within the body. For example, older individuals tend to experience higher heat strain (Hellon and Lind, 1956; Wagner et al., 1972) due to factors such as decreased sweat secretion rates, reduced cardiac output, diminished skin blood flow, and delayed onset of sweating. Furthermore, advanced models, such as the 3D anatomic thermoregulation model, can provide highly detailed temperature distributions within the human body, making them particularly useful for medical applications, such as assessing temperature at the organ level or specific body locations; capabilities that are not possible with simplified models. In this study, the mean skin temperature data used for validation were sourced from multiple studies in the literature. These studies may have employed different methods to calculate mean skin temperature, utilizing various weighing factors and different sets of body segments for measurement. For instance, some studies computed mean skin temperature based on a weighted average of 4 or 7 body segments (Hardy et al., 1938; RAMANATHAN, 1964). These variations in methods introduce an uncertainty of ±0.4°C (95% confidence interval) (Choi et al., 1997). However, this uncertainty is considered negligible during the validation process, as it falls within the acceptable threshold of 1.6°C. In the simulations conducted for this study, mean skin temperature is calculated using the area-weighted average temperature of skin segments.

Additionally, the performance of these models cannot be extrapolated to cold exposure scenarios. In cold environments, reduced blood flow to extremities increases the risk of major cold injuries, such as frostbite, which primarily affect the fingers, toes, and other extremities (Forster et al., 1946; Sullivan-Kwantes et al., 2019). Therefore, 3D thermoregulation models that incorporate detailed blood flow through Arteriovenous Anastomoses (AVA) and include anatomical features of the extremities are more suitable for simulating cold exposure conditions (Fallahi et al., 2017; Gorgas et al., 1977; Rida et al., 2014; Yang et al., 2017; Zhang et al., 2024, 2021). Furthermore, all the evaluated models use a simplified clothing model that does not account for wet conduction or sweat accumulation in the clothing. This limitation can impact the accuracy of predicted skin temperature and total heat transfer at skin/clothing surface (Joshi et al., 2023b), especially during transitional conditions—such as moving from a hot, humid environment to a dry one—an effect observed around the 200th minute in Case 4 (Figure 3 and Table 2).

5. Conclusions

The comparative validation of five thermoregulation models with varying levels of complexity, including the updated Stolwijk-2024 model, demonstrates that multi-node and multi-segment models are highly effective in simulating physiological heat strain across a wide range of climatic conditions. The study's findings highlight the robust predictive performance of the JOS3, UTCI-Fiala, and Stolwijk-2024 models, with these models achieving low RMSD values and minimal bias in predicting core and skin temperatures. The Stolwijk-2024 model, which incorporates updated set-point temperatures, improved heat transfer coefficients, and refined efferent control signals, shows significant improvements over the original Stolwijk-1971 model. Despite its simplified approach to modeling blood flow and heat transfer, the Stolwijk-2024 model delivers reliable predictions that are comparable to more complex models like JOS3 and UTCI-Fiala. This study indicates that while increased complexity can enhance accuracy slightly (by less than 0.1°C in core temperature), well-designed simplified models can still provide highly accurate results for specific applications.

The study also underscores the importance of using multi-node and multi-segment models for analyzing heat strain under diverse conditions, including extreme dry-heat, humid-heat, transient heat exposures, and varying levels of physical activity and clothing insulation. However, the study also identifies limitations in simpler models like the Stolwijk-1971 and Gagge two-node models, particularly in scenarios involving high metabolic rates and extreme heat. Stolwijk-1971 model tends to underpredict core temperatures, which could lead to a false sense of safety in real-world applications. This underlines the need for caution when applying such models in high heat-strain environments.

In summary, the validated multi-node and multi-segment thermoregulation models, particularly with the source-code such as JOS3 and Stolwijk-2024 models, provide reliable and accessible tools for assessing heat strain and thermal comfort in moderate to extreme environmental conditions. Future research should focus on further refining these models, addressing their limitations, and improving their accessibility to ensure they can be effectively utilized in assessing heat-strain at individual levels in a wide range of applications, from public health interventions to climate resilience planning.

References

Castellani, M.P., Rioux, T.P., Castellani, J.W., Potter, A.W., Xu, X., 2021. A geometrically accurate 3 dimensional model of human thermoregulation for transient cold and hot environments. Comput Biol Med 138. https://doi.org/10.1016/j.compbiomed.2021.104892

Choi, J.K., Miki, K., Sagawa, S., Shiraki, K., 1997. Evaluation of mean skin temperature formulas by infrared thermography. Int J Biometeorol 41, 68–75. https://doi.org/10.1007/S004840050056/METRICS

Cissé, G., McLeman, R., Adams, H., Aldunce, P., Bowen, K., 2022. 2022: health, wellbeing, and the changing structure of communities.

Davoodi, F., Hassanzadeh, H., Zolfaghari, S.A., Havenith, G., Maerefat, M., 2018. A new individualized thermoregulatory bio-heat model for evaluating the effects of personal characteristics on human body thermal response. Build Environ 136, 62–76. https://doi.org/10.1016/j.buildenv.2018.03.026

Deng, Q., Zhao, J., Liu, W., Li, Y., 2018. Heatstroke at home: Prediction by thermoregulation modeling. Build Environ 137, 147–156. https://doi.org/10.1016/j.buildenv.2018.04.017

Dongmei, P., Mingyin, C., Shiming, D., Minglu, Q., 2012. A four-node thermoregulation model for predicting the thermal physiological responses of a sleeping person. Build Environ 52, 88–97. https://doi.org/10.1016/J.BUILDENV.2011.12.020

Ebi, K.L., Capon, A., Berry, P., Broderick, C., De Dear, R., Havenith, G., Honda, Y., Kovats, S., Ma, W., Malik, A., Morris, N.B., Nybo, L., Seneviratne, S.I., Vanos, J., Jay, O., 2021. Hot weather and heat extremes: health risks. The Lancet 398, 698–708. https://doi.org/10.1016/S0140-6736(21)01208-3

Ebi, K.L., Vanos, J., Baldwin, J.W., Bell, J.E., Hondula, D.M., Errett, N.A., Hayes, K., Reid, C.E., Saha, S., Spector, J., Berry, P., 2020. Extreme Weather and Climate Change: Population Health and Health System Implications. Annu Rev Public Health 42, 293–315. https://doi.org/10.1146/ANNUREV-PUBLHEALTH-012420-105026

Fallahi, A., Salimpour, M.R., Shirani, E., 2017. A 3D thermal model to analyze the temperature changes of digits during cold stress and predict the danger of frostbite in human fingers. J Therm Biol 65, 153–160. https://doi.org/10.1016/J.JTHERBIO.2017.03.001

Fiala, D., Havenith, G., Bröde, P., Kampmann, B., Jendritzky, G., 2012. UTCI-Fiala multi-node model of human heat transfer and temperature regulation. Int J Biometeorol 56, 429–441.

Forster, R.E., Ferris, B.G., Day, R., 1946. The relationship between total heat exchange and blood flow in the hand at various ambient temperatures. Am J Physiol 146, 600–609. https://doi.org/10.1152/AJPLEGACY.1946.146.4.600

Gagge, A.P., 1971. An effective temperature scale based on a simple model of human physiological regulatory response. Ashrae Trans. 77, 247–262.

Gonzalez, R.R., Mclellan, T.M., Withey, W.R., Chang, S.K., Pandolf, K.B., 1997. Heat strain models applicable for protective clothing systems: comparison of core temperature response. J Appl Physiol (1985) 83, 1017–1032. https://doi.org/10.1152/JAPPL.1997.83.3.1017

Gordon, R.G., Roemer, R.B., Horvath, S.M., 1976. A Mathematical Model of the Human Temperature Regulatory System–Transient Cold Exposure Response. IEEE Trans Biomed Eng BME-23, 434–444. https://doi.org/10.1109/TBME.1976.324601

Gorgas, K., Böck, P., Tischendorf, F., Currî, S.B., 1977. The fine structure of human digital arterio-venous anastomoses (Hoyer-Grosser's organs). Anat Embryol (Berl) 150, 269–289. https://doi.org/10.1007/BF00318346

Hardy, J.D., Du Bois, E.F., Soderstrom, G.F., 1938. The Technic of Measuring Radiation and Convection: One Figure. J Nutr 15, 461–475. https://doi.org/10.1093/JN/15.5.461

Haslam, R.A., Parsons, K.C., 1994. Using computer-based models for predicting human thermal responses to hot and cold environments. Ergonomics 37, 399–416. https://doi.org/10.1080/00140139408963659

Haslam, R.A., Parsons, K.C., 1988. An evaluation of computer-based models that predict human responses to the thermal environment. ASHRAE Trans 94, e60.

Havenith, G., 2001. Individualized model of human thermoregulation for the simulation of heat stress response. J Appl Physiol (1985) 90, 1943–1954. https://doi.org/10.1152/JAPPL.2001.90.5.1943

Havenith, George., 1997. Individual heat stress response. [Katholieke Universiteit Nijmegen].

Hellon, R.F., Lind, A.R., 1956. Observations on the activity of sweat glands with special reference to the influence of ageing. J Physiol 133, 132. https://doi.org/10.1113/JPHYSIOL.1956.SP005571

Huizenga, C., Hui, Z., Arens, E., 2001. A model of human physiology and comfort for assessing complex thermal environments. Build Environ 36, 691–699. https://doi.org/10.1016/S0360-1323(00)00061-5

Intergovernmental Panel on Climate Change (IPCC), 2019. Global Warming of 1.5° C. An IPCC Special Report on the impacts of global warming of 1.5° C above pre-industrial levels and related global greenhouse gas emission pathways, in the context of strengthening the global response to the threat of climate change. Ed. by Masson-Delmotte V, Zhai P, Portner HO, et al. ipcc Geneva.

Jack, A., 2009. Einfluss hoch funktioneller Sporttextilien auf die Thermoregulation von Ausdauerathleten bei unterschiedlichen Umgebungstemperaturen. Universität Bayreuth / Kulturwissenschaftliche Fakultät.

Jay, O., Capon, A., Berry, P., Broderick, C., De Dear, R., Havenith, G., Honda, Y., Kovats, S., Ma, W., Malik, A., Morris, N.B., Nybo, L., Seneviratne, S.I., Vanos, J., Ebi, K.L., 2021. Reducing the health effects of hot weather and heat extremes: from personal cooling strategies to green cities. The Lancet 398, 709–724. https://doi.org/10.1016/S0140-6736(21)01209-5

Jendritzky, G., de Dear, R., Havenith, G., 2012. UTCI-Why another thermal index? Int J Biometeorol 56, 421–428. https://doi.org/10.1007/s00484-011-0513-7

Joshi, A., Bartels, L., Viswanathan, S.H., Martinez, D.M., Sadeghi, K., Jaiswal, A.K., Collins, D., Rykaczewski, K., 2023a. Evaluation of thermal properties and thermoregulatory impacts of lower back exosuit using thermal manikin. Int J Ind Ergon 98, 103517.

Joshi, A., Psikuta, A., Bueno, M.A., Annaheim, S., Rossi, R.M., 2023b. Modelling of heat and mass transfer in clothing considering evaporation, condensation, and wet conduction with case study. Build Environ 228, 109786. https://doi.org/10.1016/J.BUILDENV.2022.109786

Joshi, A., Wang, F., Kang, Z., Yang, B., Zhao, D., 2022. A three-dimensional thermoregulatory model for predicting human thermophysiological responses in various thermal environments. Build Environ 207. https://doi.org/10.1016/j.buildenv.2021.108506

Kaciuba-Uscilko, H., Grucza, R., 2001. Gender differences in thermoregulation. Curr Opin Clin Nutr Metab Care 4, 533–536.

Kang, Z., Wang, F., Udayraj, 2019. An advanced three-dimensional thermoregulation model of the human body: Development and validation. International Communications in Heat and Mass Transfer 107, 34–43. https://doi.org/10.1016/J.ICHEATMASSTRANSFER.2019.05.006

Karanja, J., Vanos, J., Joshi, A., Penner, S., Guzman, G.E., Connor, D.S., Rykaczewski, K., 2024. Impact of tent shade on heat exposures and simulated heat strain for people experiencing homelessness. Int J Biometeorol. https://doi.org/10.1007/S00484-024-02751-0

Matsumoto, T., Miyawaki, T., Ue, H., Kanda, T., Zenji, C., Moritani, T., 1999. Autonomic responsiveness to acute cold exposure in obese and non-obese young women. International Journal of Obesity 1999 23:8 23, 793–800. https://doi.org/10.1038/sj.ijo.0800928

Moran, D.S., Shitzer, A., Pandolf, K.B., 1998. A physiological strain index to evaluate heat stress. Am J Physiol 275. https://doi.org/10.1152/AJPREGU.1998.275.1.R129

Munir, A., Takada, S., Matsushita, T., 2009. Re-evaluation of Stolwijk's 25-node human thermal model under thermal-transient conditions: Prediction of skin temperature in low-activity conditions. Build Environ 44, 1777–1787. https://doi.org/10.1016/j.buildenv.2008.11.016

Nelson, D.A., Charbonnel, S., Curran, A.R., Marttila, E.A., Fiala, D., Mason, P.A., Ziriax, J.M., 2009. A high-resolution voxel model for predicting local tissue temperatures in humans subjected to warm and hot environments. J Biomech Eng 131. https://doi.org/10.1115/1.3002765/459859

Ooka, R., Minami, Y., Sakoi, T., Tsuzuki, K., Rijal, H.B., 2010. Improvement of sweating model in 2-Node Model and its application to thermal safety for hot environments. Build Environ 45, 1565–1573. https://doi.org/10.1016/J.BUILDENV.2009.12.012

Ou, Y., Wang, F., Zhao, J., Deng, Q., 2023. Risk of heatstroke in healthy elderly during heatwaves: A thermoregulatory modeling study. Build Environ 237, 110324. https://doi.org/10.1016/J.BUILDENV.2023.110324

Perkins-Kirkpatrick, S.E., Gibson, P.B., 2017. Changes in regional heatwave characteristics as a function of increasing global temperature. Sci Rep 7, 12256.

Psikuta, A., Fiala, Dusan, Laschewski, Gudrun, Jendritzky, Gerd, Richards, Mark, Błażejczyk, Krzysztof, Mekjavič, I., Rintamäki, Hannu, Richards, M, Fiala, D, Laschewski, G, Jendritzky, G, Błażejczyk, K, Rintamäki, H, Havenith, G., 2012. Validation of the Fiala multi-node thermophysiological model for UTCI application. Int J Biometeorol 56, 443–460. https://doi.org/10.1007/s00484-011-0450-5

RAMANATHAN, N.L., 1964. A new weighting system for mean surface temperature of the human body. https://doi.org/10.1152/jappl.1964.19.3.531 19, 531–533. https://doi.org/10.1152/JAPPL.1964.19.3.531

Rida, M., Karaki, W., Ghaddar, N., Ghali, K., Hoballah, J., 2014. A new mathematical model to simulate AVA cold-induced vasodilation reaction to local cooling. Int J Biometeorol 58, 1905–1918. https://doi.org/10.1007/S00484-014-0792-X

Roelofsen, P., Jansen, K., Vink, P., 2023. A transient thermal sensation equation fit for the modified Stolwijk model. Intelligent Buildings International. https://doi.org/10.1080/17508975.2021.1962785

Roelofsen, P., Vink, P., 2016. Improvement of the Stolwijk model with regard to clothing, thermal sensation and skin temperature. Work 54, 1009–1024. https://doi.org/10.3233/WOR-162357

Silva, A.B.C.G., Wrobel, L.C., Ribeiro, F.L.B., 2018. A thermoregulation model for whole body cooling hypothermia. J Therm Biol 78, 122–130. https://doi.org/10.1016/J.JTHERBIO.2018.08.019

Smallcombe, J.W., Foster, J., Hodder, S.G., Jay, O., Flouris, A.D., Havenith, · George, 2022. Quantifying the impact of heat on human physical work capacity; part IV: interactions between work duration and heat stress severity. Springer 1, 3. https://doi.org/10.1007/s00484-022-02370-7

Song, W., Wang, F., Zhang, C., 2019. Intermittent wetting clothing as a cooling strategy for body heat strain alleviation of vulnerable populations during a severe heatwave incident. J Therm Biol 79, 33–41. https://doi.org/10.1016/J.JTHERBIO.2018.11.012

Standard, A., 1992. Thermal environmental conditions for human occupancy. ANSI/ASHRAE, 55 5.

Stolwijk, J.A., 1971. A mathematical model of physiological temperature regulation in man.

Stolwijk, J.A., Hardy, J.D., 1966a. Partitional calorimetric studies of responses of man to thermal transients. J Appl Physiol 21, 967–977. https://doi.org/10.1152/JAPPL.1966.21.3.967

Stolwijk, J.A., Hardy, J.D., 1966b. Partitional calorimetric studies of responses of man to thermal transients. J Appl Physiol 21, 967–977. https://doi.org/10.1152/JAPPL.1966.21.3.967

Stolwijk, J.A.J., Hardy, J.D., 1966. Temperature regulation in man--a theoretical study. Pflugers Arch Gesamte Physiol Menschen Tiere 291, 129–162. https://doi.org/10.1007/BF00412787

Sullivan-Kwantes, W., Moes, K., Limmer, R., Goodman, L., 2019. Finger cold-induced vasodilation test does not predict subsequent cold injuries: A lesson from the 2018 Canadian Forces Exercise. Temperature: Multidisciplinary Biomedical Journal 6, 142. https://doi.org/10.1080/23328940.2019.1574200

Takada, S., Kobayashi, H., Matsushita, T., 2009. Thermal model of human body fitted with individual characteristics of body temperature regulation. Build Environ 44, 463–470. https://doi.org/10.1016/j.buildenv.2008.04.007

Takahashi, Y., Nomoto, A., Yoda, S., Hisayama, R., Ogata, M., Ozeki, Y., Tanabe, S. ichi, 2021. Thermoregulation model JOS-3 with new open source code. Energy Build 231. https://doi.org/10.1016/j.enbuild.2020.110575

Tanabe, S.I., Kobayashi, K., Nakano, J., Ozeki, Y., Konishi, M., 2002. Evaluation of thermal comfort using combined multi-node thermoregulation (65MN) and radiation models and computational fluid dynamics (CFD). Energy Build 34, 637–646. https://doi.org/10.1016/S0378-7788(02)00014-2

Tang, Y., Yu, H., Wang, Z., Luo, M., Energies, C.L.-, 2020, undefined, 2020. Validation of the Stolwijk and Tanabe human thermoregulation models for predicting local skin temperatures of older people under thermal transient conditions. mdpi.comY Tang, H Yu, Z Wang, M Luo, C LiEnergies, 2020•mdpi.com. https://doi.org/10.3390/en13246524

Tartarini, F., Schiavon, S., Cheung, T., Hoyt, T., 2020. CBE Thermal Comfort Tool: Online tool for thermal comfort calculations and visualizations. SoftwareX 12, 100563. https://doi.org/10.1016/J.SOFTX.2020.100563

Trenberth, K.E., Dai, A., Rasmussen, R.M., Parsons, D.B., 2003. The changing character of precipitation. Bull Am Meteorol Soc 84, 1205–1218.

Van Marken Lichtenbelt, W.D., Frijns, A.J.H., Van Ooijen, M.J., Fiala, D., Kester, A.M., Van Steenhoven, A.A., 2007. Validation of an individualised model of human thermoregulation for predicting responses to cold air. Int J Biometeorol 51, 169–179. https://doi.org/10.1007/S00484-006-0060-9/FIGURES/4

Van Someren, E.J.W., Raymann, R.J.E.M., Scherder, E.J.A., Daanen, H.A.M., Swaab, D.F., 2002. Circadian and age-related modulation of thermoreception and temperature regulation: mechanisms and functional implications. Ageing Res Rev 1, 721–778. https://doi.org/10.1016/S1568-1637(02)00030-2

Vanos, J., Guzman-Echavarria, G., Baldwin, J.W., Bongers, C., Ebi, K.L., Jay, O., 2023. A physiological approach for assessing human survivability and liveability to heat in a changing climate. Nat Commun 14. https://doi.org/10.1038/s41467-023-43121-5

Vanos, J.K., Joshi, A., Guzman-Echavarria, G., Rykaczewski, K., Hosokawa, Y., 2024. Impact of Reflective Roadways on Simulated Heat Strain at the Tokyo, Paris and Los Angeles Olympics. Journal of Science in Sport and Exercise. https://doi.org/10.1007/S42978-024-00294-9

Wagner, J.A., Robinson, S., Tzankoff, S.P., Marino, R.P., 1972. Heat tolerance and acclimatization to work in the heat in relation to age. https://doi.org/10.1152/jappl.1972.33.5.616 33, 616–622. https://doi.org/10.1152/JAPPL.1972.33.5.616

Wissler, E.H., 2018. Temperature Distribution in the Body. Human Temperature Control 265–287. https://doi.org/10.1007/978-3-662-57397-6_7

Yang, J., Weng, W., Wang, F., Song, G., 2017. Integrating a human thermoregulatory model with a clothing model to predict core and skin temperatures. Appl Ergon 61, 168–177. https://doi.org/10.1016/j.apergo.2017.01.014

Zhang, H., Huizenga, C., Arens, E., Yu, T., 2001. Considering individual physiological differences in a human thermal model. J Therm Biol 26, 401–408. https://doi.org/10.1016/S0306-4565(01)00051-1

Zhang, M., Li, R., Li, J., Wang, F., Subramaniam, S., Lang, J., Passalacqua, A., Song, G., 2021. A 3D multi-segment thermoregulation model of the hand with realistic anatomy: Development, validation, and parametric analysis. Build Environ 201. https://doi.org/10.1016/j.buildenv.2021.107964

Zhang, M., Li, R., Wu, Y., Song, G., 2024. Thermoregulation of human hands in cold environments and its modeling approach: A comprehensive review. Build Environ 248, 111093. https://doi.org/10.1016/J.BUILDENV.2023.111093

Zhao, J., Wang, H., Li, Y., Xiao, F., Deng, Q., 2020. Heatstroke recovery at home as predicted by human thermoregulation modeling. Build Environ 173. https://doi.org/10.1016/j.buildenv.2020.106752